JOURNAL OF VIROLOGY, Nov. 2005, p. 13463–13472 Vol. 79, No. 21
0022-538X/05/$08.00+0 doi:10.1128/JVI.79.21.13463–13472.2005


# The Retroviral Capsid Domain Dictates Virion Size, Morphology, and Coassembly of Gag into Virus-Like Particles

Danso Ako-Adjei, Marc C. Johnson, and Volker M. Vogt*

*Department of Molecular Biology and Genetics, Cornell University, Ithaca, New York 14853*

Received 12 April 2005/Accepted 3 August 2005

**The retroviral structural protein, Gag, is capable of independently assembling into virus-like particles (VLPs) in living cells and in vitro. Immature VLPs of human immunodeficiency virus type 1 (HIV-1) and of Rous sarcoma virus (RSV) are morphologically distinct when viewed by transmission electron microscopy (TEM). To better understand the nature of the Gag-Gag interactions leading to these distinctions, we constructed vectors encoding several RSV/HIV-1 chimeric Gag proteins for expression in either insect cells or vertebrate cells. We used TEM, confocal fluorescence microscopy, and a novel correlative scanning EM (SEM)-confocal microscopy technique to study the assembly properties of these proteins. Most chimeric proteins assembled into regular VLPs, with the capsid (CA) domain being the primary determinant of overall particle diameter and morphology. The presence of domains between matrix and CA also influenced particle morphology by increasing the spacing between the inner electron-dense ring and the VLP membrane. Fluorescently tagged versions of wild-type RSV, HIV-1, or murine leukemia virus Gag did not colocalize in cells. However, wild-type Gag proteins colocalized extensively with chimeric Gag proteins bearing the same CA domain, implying that Gag interactions are mediated by CA. A dramatic example of this phenomenon was provided by a nuclear export-deficient chimera of RSV Gag carrying the HIV-1 CA domain, which by itself localized to the nucleus but relocalized to the cytoplasm in the presence of wild type HIV-1 Gag. Wild-type and chimeric Gag proteins were capable of coassembly into a single VLP as viewed by correlative fluorescence SEM if, and only if, the CA domain was derived from the same virus. These results imply that the primary selectivity of Gag-Gag interactions is determined by the CA domain.**

In retroviruses, the *gag* gene encodes the major structural polyprotein, which is necessary and sufficient for the assembly and release of virus-like particles (VLPs). Molecules of the Gag protein by themselves can interact to form a complete virus particle (assembly), but release of the particle from the cell (budding) is a separate process that requires cellular factors (20). While Gag proteins vary in size and show almost no sequence identity across genera, they share at least three major domains. These domains, matrix (MA), capsid (CA), and nucleocapsid (NC), are separated by proteolytic cleavage sites that are acted on by the viral protease during or shortly after the release of nascent particles. Proteolytic cleavage triggers morphological changes known as maturation. In addition to liberating the major Gag domains, cleavage also generates several shorter peptides. In alpharetroviruses such as Rous sarcoma virus (RSV), these include p2, p10, and SP, while in the lentivirus human immunodeficiency virus type 1 (HIV-1), they include SP1, SP2, and p6.

During assembly, each Gag domain plays important structural and functional roles. The MA domain targets Gag to the plasma membrane. In RSV, this process is mediated by positively charged residues (9, 16), while in HIV-1 and most other retroviruses it is also mediated by a myristate modification. The NC domain contains one or two zinc finger-like cysteine-histidine (Cys-His) motifs, flanked by clusters of basic residues (1, 40), which together act to coordinate interactions with the viral genomic RNA. NC is also capable of binding nonspecifically to RNAs. During assembly, the CA domain is thought to play a key role in Gag-Gag interactions (22–24, 38, 43, 54, 63), although both MA-MA and NC-NC domain interactions have also been suggested to be involved (57, 64, 69). While the exact nature of CA-CA domain contacts in immature particles is not known, in mature particles the CA lattice has been modeled based on crystal structures and on cryo-electron microscopy (cryo-EM) reconstruction of CA tubes assembled in vitro or purified from mature virions (8, 23, 45). In the model, six CA N-terminal domains (NTD) form a hexagonal ring, and each ring is connected to six neighboring rings by a dimer interface between two C-terminal domains (CTD), thus forming a lattice. It is unclear to what extent the mature CA-CA interactions mimic those in immature assembly of Gag particles.

Although CA proteins share significant sequence similarity in only a small region known as the major homology region (MHR), the tertiary structures of all solved retroviral CA domains are remarkably similar (11, 22, 28, 32, 37, 38, 54). Although the structures of MA proteins are somewhat less conserved, they are recognizably similar as well (14, 50–53); in some cases, MA domains are functionally interchangeable between retroviruses (3, 17, 18, 36). Similarly, in some cases NC domains have been exchanged without compromising assembly (21). The studies that sought to determine whether CA domains are also interchangeable (18, 66) focused on infectivity and did not address the morphological effects of CA exchange. Although both MA and NC demonstrate functional conservation, few detailed comparisons of virion size and morphology across genera have been carried out to address whether functional equivalence leads to the same physical characteristics of the VLPs. For instance, although cryo-EM and thin-section

* Corresponding author. Mailing address: Department of Molecular Biology and Genetics, Cornell University, Ithaca, NY 14853. Phone: (607) 255-2443. Fax: (607) 255-2428. E-mail: vmv1@cornell.edu.

transmission EM (TEM) measurements are available for RSV and HIV-1 (39, 65), only two reports directly compared wild-type and domain-exchanged VLPs in the same experiment (34, 36).

The Gag domain(s) that dictates particle size and morphology is not well defined. Unlike the mature forms of the virus, which by thin-section EM appear distinctly different in viruses of different genera, immature VLPs all display the same general morphology, with a single inner electron-dense ring. Therefore, the only dimensions that determine the morphology of an immature VLP are the diameter of this dark inner ring, the overall diameter of the particle, and the ratio of these two diameters. We have observed previously that immature HIV-1 VLPs are larger (both in inner ring and overall diameters) than immature RSV VLPs and also appear morphologically distinct, with their dark inner ring seeming much farther from the particle center. To determine the origin of these differences in size and morphology and to address the role of domain contacts in Gag assembly, we created expression constructs for a series of chimeric RSV/HIV-1 proteins. The resulting VLPs produced in a baculovirus-insect cell expression system and in transfected vertebrate cells were characterized by thin-section TEM, confocal fluorescence microscopy, and correlative scanning EM-confocal microscopy. The results imply that the CA domain, together with short adjoining sequences, carries the primary determinants of retroviral morphology.

## MATERIALS AND METHODS

**Construction of chimeric VLPs and plasmids.** All chimeras were constructed by mutagenic PCR and placed downstream of the *Autographa californica* nuclear polyhedrosis virus polyhedron promoter with the appropriate restriction sites. The chimeric Gag coding region was first built into the pFastBac donor plasmid and transposed into the baculovirus genome with the Bac-to-Bac system (Invitrogen). Colonies with successful transpositions were selected by screening on Luria agar plates containing 50-μg/ml kanamycin, 70-μg/ml gentamicin, 10-μg/ml tetracycline, 100-μg/ml Blue-Gal, and 40-μg/ml isopropyl-ā-D-thiogalactopyranoside (IPTG). RSV sequences were derived from the Prague C strain of RSV. Chimeric HIV-1 constructs were derived from the pNL4-3 and HXB2 strains. The wild-type HIV-1 construct used in the DF1 analysis was derived from plasmid pGag-EGFP (31).

RH consists of RSV MA-p2-p10-CA-SP fused to HIV-1 NC-SP2 (RSV $Gag_{1–488}$ and HIV-1 $Gag_{378–448}$). HR consists of HIV-1 MA-CA-SP1 fused to RSV NC (HIV-1 $Gag_{1–377}$ and RSV $Gag_{489–578}$). RHR consists of RSV MA-p2-p10 followed by HIV-1 CA-SP1 fused to RSV NC (RSV $Gag_{1–239}$, HIV-1 $Gag_{133–377}$, and RSV $Gag_{489–578}$). HRH2 consists of HIV-1 MA followed by the last 25 amino acids from RSV p10-CA-SP fused to HIV-1 NC-SP2 (HIV-1 $Gag_{1–132}$, RSV $Gag_{215–488}$, and HIV-1 $Gag_{378–448}$). RHR2 consists of RSV MA followed by the last 25 amino acids of HIV-1 MA, and HIV-1 CA-SP1 fused to RSV NC (RSV $Gag_{1–155}$, HIV-1 $Gag_{108–377}$, and RSV $Gag_{489–578}$). HRH consists of HIV-1 MA followed by RSV CA-SP fused to HIV-1 NC-SP2 (HIV-1 $Gag_{1–132}$, RSV $Gag_{240–488}$, and HIV-1 $Gag_{378–448}$). RnHc consists of RSV MA-CA NTD fused to HIV-1 CTD-SP1-NC-SP2 (RSV $Gag_{1–393}$ and HIV-1 $Gag_{284–448}$). HnRc consists of HIV-1 MA-CA NTD fused to RSV CTD-SP-NC (HIV-1 $Gag_{1–283}$ and RSV $Gag_{394–578}$). Constructed in this fashion, the CTD of RnHc and HnRc begin with the first residue of the MHR (Asp). HIV-1, RSV, and chimeric Gag fluorescent constructs were placed upstream of the *Aequorea victoria* enhanced green fluorescent protein (designated EGFP) variants cyan fluorescent protein (CFP) and yellow fluorescent protein (YFP) (Clontech). Murine leukemia virus (MLV) clones were obtained from Walther Mothes (Yale University School of Medicine). The wild-type fluorescent HIV-1 construct was obtained from Marilyn Resh (Memorial Sloan-Kettering Cancer Center). The structures of all of the Gag proteins used in this study are diagrammed in Fig. 1.

**Cell culture and transfection.** *Spodoptera frugiperda* cells (SF9) were maintained in suspension at 27°C in SF900-II serum-free medium (Invitrogen). Mid-log-phase SF9 cells were seeded at $10^6$ cells per 35-mm plate in 2 ml of SF900-II serum-free medium containing 50-μg/ml penicillin and 50-μg/ml streptomycin. Seeded SF9 cells were transfected with isolated recombinant bacmids using CellFECTIN reagent (Invitrogen) according to the manufacturer's instructions. Recombinant baculovirus was harvested from supernatant 72 h posttransfection and used to infect SF9 cells growing in suspension at 27°C. Infected Sf9 cells were fixed for EM analysis 48 h postinfection. DF-1 chicken fibroblast cells were grown in Dulbecco's modified Eagle's medium augmented with 10% fetal bovine serum, 1% heat-inactivated chick serum, and 1% (each) of concentrated stocks of glutamine and vitamin mix (Invitrogen). DF-1 cells were transfected with FuGENE 6 (Roche) according to the manufacturer's instructions. For the confocal and correlative SEM-confocal analysis, DF-1 cells transfected with fluorescent RSV or HIV-1 Gag constructs were also transfected with the homologous nonfluorescently labeled wild-type Gag constructs at a ratio of 1:4 (fluorescent Gag:nonfluorescent Gag) to allow proper assembly.

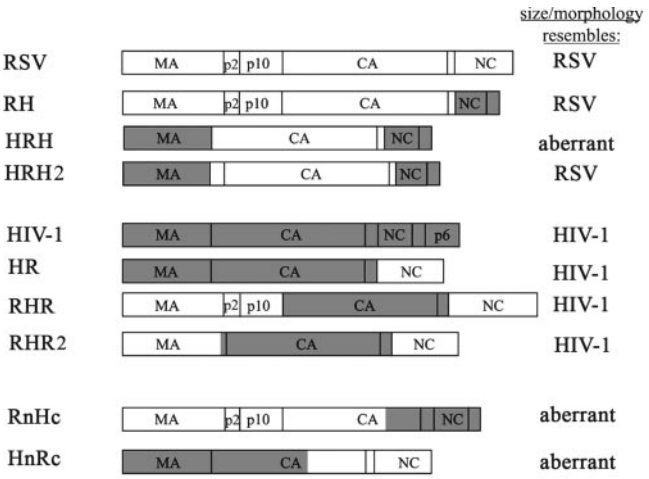


FIG. 1. Schematic diagram and descriptions of wild-type and chimeric RSV/HIV-1 Gag proteins and summary of phenotype. RSV domains are in white; HIV-1 domains are in gray.

**Transmission electron microscopy.** Infected SF9 cells were collected 48 h postinfection, fixed with 2.5% glutaraldehyde in Sorensen's Na-K phosphate buffer (29% 0.066 M $KH_2PO_4$, 71% 0.066 M $Na_2HPO_4$, pH 7.2) and treated with 2% osmium tetraoxide as a secondary fixative. Samples were then dehydrated in a series of ethanol washes. Cells or VLPs collected through a sucrose cushion were embedded in Spurr's low-viscosity embedding mixture (61) according to the manufacturer's instructions (Electron Microscopy Sciences). Spurr sections were placed on 400-mesh square copper EM grids (Electron Microscopy Sciences), stained with 2% uranyl acetate followed by secondary staining with 0.1% lead citrate, and viewed with a Philips 301 TEM. For statistical analysis, the unpaired *t* test was used to compare the values of the means from wild-type and chimeric VLPs. Calculations were carried out with GraphPad software (www.graphpad.com).

**Confocal fluorescence microscopy and correlative SEM-confocal microscopy.** Confocal laser scanning microscopy was performed with a Leica TCS SP2 microscope. All images were collected with a 100×, 1.40 numerical aperture oil immersion lens unless otherwise mentioned. Cells were fixed 20 to 24 h posttransfection with 4% paraformaldehyde and washed with standard phosphate-buffered saline prior to being mounted in Fluoromount-G (Electron Microscopy Sciences). An argon laser with excitation wavelengths of 458 nm and 514 nm was used for CFP and YFP, respectively. Images were analyzed with Leica Confocal Software (Leica Microsystems) or Adobe Photoshop CS (Adobe Systems). VLPs used for correlative SEM-confocal microscopy analysis were washed with phosphate-buffered saline and mildly fixed in 4% paraformaldehyde for 10 min prior to confocal analysis. After fluorescence imaging, VLPs were further fixed in 2% glutaraldehyde, postfixed with osmium tetraoxide, and finally dehydrated in a series of ethanol washes in preparation for SEM analysis. Samples were then critical point dried, sputter coated with a thin layer of gold-palladium, and viewed on an LEO 1550 field emission scanning electron microscope at 3 keV.

## RESULTS

It was reported previously that HIV-1 and RSV VLPs from a baculovirus expression system differ in appearance (34). To illustrate this difference directly, we thin sectioned a mixed

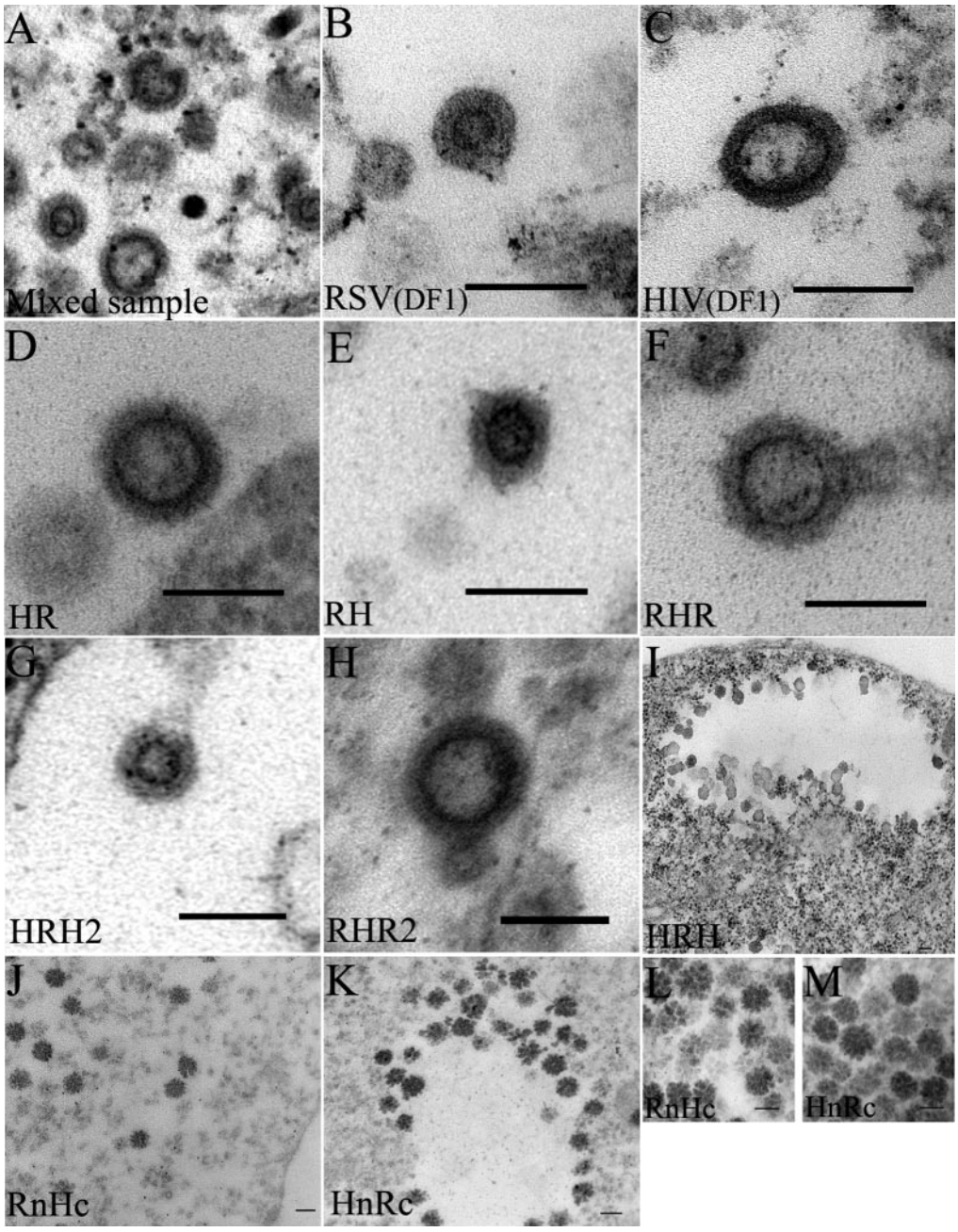


FIG. 2. Thin-section TEM of wild-type and chimeric RSV/HIV-1 VLPs. (A) Pellet from mixed medium collected from SF9 cells expressing RSV and HIV-1 Gag. (B and C) Pellets from medium collected from DF1 cells expressing Gag proteins by transient transfection. (D to M) SF9 cells expressing Gag proteins by baculovirus infection. Wild-type RSV Gag (B); wild-type HIV-1 Gag (C); HR (D); RH (E); RHR (F); HRH2 (G); pellet from medium collected from SF9 cells expressing RHR2 (H); HRH (I); RnHc (J); HnRc (K); high magnification of RnHc (L); high magnification of HnRc (M). Scale bars, 100 nm.

pellet of baculovirus-derived HIV-1 and RSV VLPs (Fig. 2A). In agreement with the previous report, the diameters of the dark inner rings within VLPs from HIV-1 were approximately two times larger than those from RSV, while the overall diameters of the HIV-1 particles were about one-third larger. Together, these differences made the HIV-1 VLPs appear morphologically distinct because the inner rings seemed much closer to the edge of the particles. To verify that the observed differences between RSV and HIV-1 were not an artifact of the baculovirus expression system, the two types of Gag protein were expressed in a chicken fibroblast cell line, and the resulting VLPs were thin sectioned and viewed by TEM. As with the baculovirus-derived particles, there was a discernible difference in size and morphology between HIV-1 and RSV VLPs (Fig. 2B and C and Table 1). Therefore, we conclude that these differences result from intrinsic properties of the Gag proteins.

**MA and NC do not affect the ultrastructure of RSV/HIV-1 chimeric VLPs.** Through its interactions with nucleic acid, the

TABLE 1. Summary of VLP measurements

| Name (*n*) | Origin of CA domain | Inner ring diam (nm) | VLP diam (nm) | Residues upstream of CA[b] | Outer-to-inner spacing (nm)[c] | Outer-to-inner ratio[d] |
|---|---|---|---|---|---|---|
| RSV (Bac) (41)[a] | RSV | 40 ± 2.4 | 84 ± 3.9 | 239 | 22 | 2.1 |
| RSV (DF1) (39) | RSV | 42 ± 2.8 | 84 ± 4.6 | 239 | 21 | 2.0 |
| RH (44) | RSV | 42 ± 2.1 | 82 ± 2.1 | 239 | 20 | 2.0 |
| HRH2 (48) | RSV | 46 ± 2.6 | 82 ± 3.2 | 157 | 18 | 1.8 |
| HIV (Bac) (43) | HIV | 77 ± 5.3 | 110 ± 14 | 132 | 17 | 1.4 |
| HIV (DF1) (46) | HIV | 79 ± 6.2 | 114 ± 16 | 132 | 18 | 1.4 |
| HR (51) | HIV | 72 ± 5.0 | 105 ± 9.7 | 132 | 16 | 1.5 |
| RHR (54) | HIV | 71 ± 5.1 | 112 ± 12 | 239 | 21 | 1.6 |
| RHR2 (47) | HIV | 71 ± 5.4 | 105 ± 12 | 180 | 17 | 1.5 |

[a] *n*, number of VLPs measured.
[b] Numbering from first amino acid of MA.
[c] One half of the difference between two diameters.
[d] Ratio of the outer VLP diameter to the inner ring diameter.

NC domain of Gag is thought to nucleate the retroviral assembly process (3, 13, 48). NC domains of at least some retroviruses are functional equivalents that can support assembly, budding, and (in some cases) infectivity when exchanged (3, 19, 21, 68). However, certain mutations in NC have been shown to affect assembly (49). Therefore, it seemed possible that NC might influence the size of the particle. To address the role of NC in VLP structure, we first constructed chimeric Gag proteins with heterologous NC domains, beginning with the first residue of NC (Fig. 1). All Gag constructs ended with NC and therefore lacked PR (RSV) or p6 (HIV-1). RSV PR is dispensable for assembly, and it can even disrupt proper assembly in overexpression systems (34). Although HIV-1 p6 is ordinarily required for proper budding, it too is dispensable for assembly and its deletion affects neither the width nor the spacing of density layers as determined by cryoelectron microscopy (65). Nevertheless, to rule out any effect of p6 on particle size or morphology, we directly compared baculovirus-produced wild-type and p6-deficient HIV-1 VLPs and found no significant differences (data not shown).

Exchange of the NC domains had no effect on VLP structure. VLPs composed of HIV-1 MA-CA with RSV NC (HR) clearly resembled HIV-1 particles in terms of particle diameter, inner-ring diameter, and outer-to-inner diameter ratio (Fig. 2C and Table 1). Similarly, VLPs made of RSV MA-CA with HIV-1 NC (RH) resembled RSV both in size and morphology (Fig. 2D and Table 1). These results are consistent with the previously derived conclusion that the basic residues of NC (and hence the overall charge), rather than the amino acid sequence itself, are critical for assembly (5, 13, 21, 55).

**Ultrastructure of chimeric VLPs is determined by CA.** CA is an essential domain of Gag, corresponding to known density features of immature VLPs as observed by cryo-EM (65, 67), and mutations in CA are known to compromise or abrogate proper VLP assembly (2, 24, 27, 47, 63). To assess the effect of CA on VLP size and morphology, we constructed several chimeric Gag proteins that include all or part of CA. In all of the chimeras, the spacer region (SP or SP1) separating CA and NC is retained with the adjoining homologous CA domain, as this region is critical for proper Gag assembly and may interact with CA (15, 30, 41, 46, 47).

Replacement of the RSV CA-SP region by HIV-1 CA-SP1 (RHR) resulted in particles that were similar in size and inner-ring diameter to HIV-1 VLPs (Fig. 2F and Table 1). By contrast, when HIV-1 CA-SP1 was replaced by RSV CA-SP (HRH) (Fig. 2I), highly aberrant intracellular particles were observed that were never found to bud from the plasma membrane. Although roughly spherical, HRH particles were amorphous and appeared to assemble around electron-lucent, vacuole-like regions of the cell that lacked a limiting membrane. It is unlikely that the unusual targeting is responsible for this aberrant morphology, as there are no examples in which targeting impacts VLP morphology. We hypothesized that the aberrant HRH phenotype was due to the lack of RSV amino acid residues directly upstream of RSV CA. Unlike HIV-1 Gag, RSV Gag includes a stretch of 84 residues, comprising the p2 and p10 domains, between MA and CA (Fig. 1). The C-terminal 25 amino acids residues of p10 constitute a critical determinant for the assembly of spherical virions (10, 33, 35), and structural data suggest that these amino acids interact with CA (56).

To assess the influence of the sequence immediately upstream of CA, we generated two additional chimeras, HRH2 and RHR2. The first, HRH2, is the same as HRH except that it also includes the last 25 amino acid residues of p10 adjacent to RSV CA (Fig. 1). HRH2 particles were observed at the plasma membrane and were similar in size and inner-ring diameter to RSV particles (Fig. 2F and Table 1). Unlike the HRH chimera, no aberrant particles were observed. These results support the notion that the region immediately N-terminal to RSV CA interacts with CA and is critical for proper assembly.

The second chimera, RHR2, is analogous to HRH in that the 25 residues of HIV-1 MA adjacent to CA are included. Previous studies to determine if this region of HIV-1 Gag serves an function analogous to the corresponding sequence in RSV were inconclusive (29). Although Western blot analysis confirmed proper expression of RHR2 (data not shown), VLPs never were observed associated with the cell. Plasma membrane binding of RSV Gag is believed to be mediated through basic residues in the MA domain (16). Addition of two basic residues to MA results in more rapid budding (9). Because the last 25 amino acids of HIV-1 MA in RHR2 contribute an additional three net positive charges to the RSV MA domain, we hypothesized that RHR2 also may have a faster budding rate, making it difficult to observe budding VLPs on the plasma

membrane. Consistent with this hypothesis, numerous VLPs were evident in thin sections of pellets from the centrifuged medium (Fig. 2H). These particles had dark inner rings indistinguishable in size from HIV-1 VLPs and most closely resembled HIV-1 in morphology.

By an unpaired *t* test applied to the entire collection of particles with normal morphology, the inner rings of VLPs containing RSV CA were found to be significantly different ($P < 0.0001$) from those containing HIV-1 CA (Table 1). Although the diameter of the inner ring appeared to be the major feature contributing to particle size, morphology, as assessed by eye, only identifies the relative position of the ring within the particle. To address particle morphology in quantitative terms, we calculated the ratio of the diameter of the ring to that of the periphery, as well as the distance between the inner ring and the periphery, called the outer spacing. The outer spacing did not correspond with the lineage of the CA domain but did correspond approximately with the number of amino acids residues upstream of the CA domain (Table 1). For instance, although visual inspection of HRH2 particles initially suggested an outer spacing similar to that of RSV, the measurements did not confirm this impression. HRH2 particles had an outer spacing similar to that of HIV-1 VLPs. Although this difference in spacing contributes little to the overall particle diameter, it does contribute to the morphology by changing the ratio of the inner to the outer diameters. The observed difference between wild-type RSV and HIV-1 is distinctive because HIV-1 particles have both a larger inner ring (approximate 15 nm larger in radius) and a smaller outer spacing (approximately 5 nm smaller).

In summary, from this EM analysis, particle diameter is determined primarily by CA, including SP or SP1 and, in the case of RSV CA, also including the short immediately adjoining sequences N-terminal to CA. The distance between the inner ring and the particle periphery is determined, at least in part, by the number of amino acid residues between MA and CA.

**Exchange of the CA CTD leads to aberrant particle formation.** Retroviral CA proteins are made up of an N-terminal domain and a C-terminal domain. A short unstructured linker region separates the NTD from the CTD, which begins with the highly conserved MHR (11, 28, 37, 38, 54). Interactions between these two domains appear to be important for assembly of the mature core (6, 43). To determine if either domain of CA was responsible for the observed differences between HIV-1 and RSV, we swapped the CTD of RSV and HIV-1 Gag proteins, starting at the MHR, to create RnHc and HnRc (Fig. 1). Both of these chimeric Gag proteins assembled aberrantly in the cytoplasm (Fig. 2J to M), and no membrane budding was observed. What appeared to be particles of RnHc and HnRc were found as clusters of roughly spherical dense objects reminiscent of raspberries (Fig. 2J to M). Although we have not formally proven these structures to be aggregates of either chimeric Gag protein, no similar structures in uninfected insect cells were ever observed (data not shown). An exchange of CTD domains starting with the first residue of the linker region was also performed, in which the homologous linker region was included with the CTD. In this case, although Western blot analysis confirmed expression of chimeric proteins, neither aberrant nor authentic VLPs were observed (data not shown).

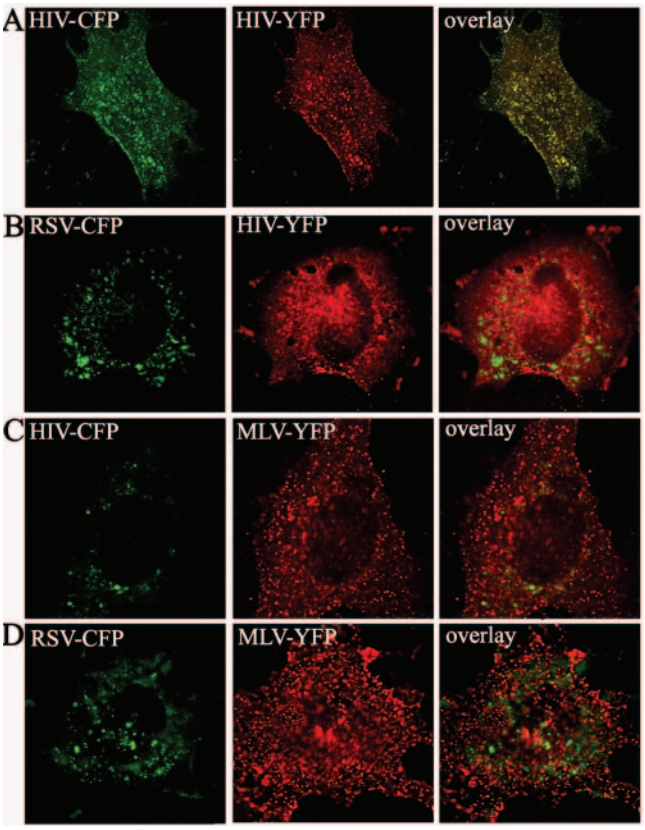


FIG. 3. Fluorescence visualization of CFP or YFP labeled RSV, HIV-1, and MLV Gag in DF1 cells. HIV-1 Gag-CFP and HIV-1 Gag-YFP (A); RSV Gag-CFP and HIV-1 Gag-YFP (B); HIV-1 Gag-CFP and MLV Gag-YFP (C); RSV Gag-CFP and MLV Gag-YFP (D). Images are pseudocolored (CFP = green; YFP = red) and represent a single focal plane.

In summary, we conclude that a species mismatch between the NTD and CTD is not conducive to proper VLP assembly.

**CA mediates coassembly of heterologous Gag proteins.** The ability of two Gag proteins to interact and coassemble might be determined by MA, CA, NC, or a combination of these domains. Our chimeric Gag proteins provided a novel means to elucidate the requirements of coassembly and to distinguish among these possibilities. First, as a control, we coexpressed pairs of fluorescently labeled RSV, HIV-1, or MLV Gag proteins in DF1 cells and examined their distribution by confocal microscopy. As expected, coexpression of the same Gag protein with different fluorescent tags led to nearly perfect colocalization, as shown for HIV-YFP/HIV-CFP (Fig. 3A). Similar results were obtained for RSV-YFP/RSV-CFP and MLV-CFP/MLV-YFP (data not shown). In contrast, coexpression of any of the three dissimilar pairs (RSV-CFP/HIV-YFP, HIV-CFP/MLV-YFP, and RSV-CFP/MLV-YFP) led to fluorescent puncta that were distinct and did not overlap (Fig. 3C and D).

Next, we analyzed cells cotransfected with different combinations of fluorescently labeled chimeric and wild-type Gag proteins. Only chimeras that were observed by TEM to assemble into VLPs resembling HIV-1 or RSV were used for this analysis. Significant colocalization was observed only for pairs containing the same CA domain. For example, HRH2-CFP

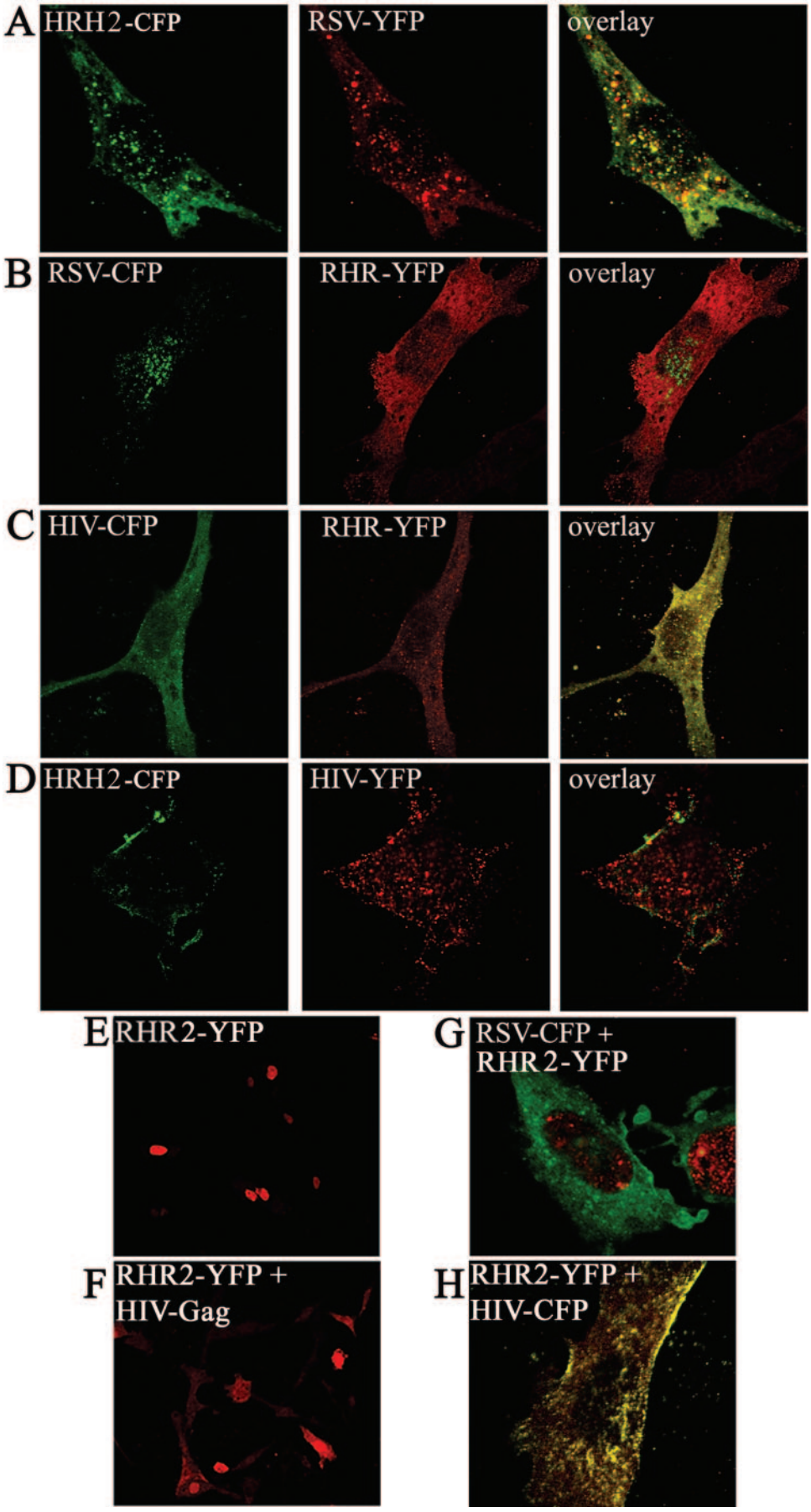
A
HRH2-CFP
RSV-YFP
overlay
B
RSV-CFP
RHR-YFP
overlay
C
HIV-CFP
RHR-YFP
overlay
D
HRH2-CFP
HIV-YFP
overlay
E
RHR2-YFP
G
RSV-CFP +
RHR2-YFP
F
RHR2-YFP +
HIV-Gag
H
RHR2-YFP +
HIV-CFP

and RSV-YFP colocalized (Fig. 4A), but RSV-CFP and RHR-YFP did not (Fig. 4B). Similarly, HIV-CFP and RHR-YFP colocalized (Fig. 4C), but HRH2-CFP and HIV-YFP did not (Fig. 4D). Interestingly, almost all of the RHR2-YFP (Fig. 4E) was retained in the nucleus. Fluorescent puncta outside the nucleus were observed in <10% of cells expressing RHR2-YFP alone. This nuclear localization is explained by the fact that the chimeric protein contains the RSV nuclear localization signal in MA but does not contain the nuclear export signal in p10 (25, 60). When RHR2-YFP was coexpressed with nonfluorescently labeled HIV-1 Gag, the cellular distribution of the fluorescent protein became predominantly extranuclear (Fig. 4F). Similarly, when RHR2-YFP and HIV-CFP were coexpressed, more than three-quarters of the cells with detectable amounts of both proteins showed colocalization outside the nucleus (Fig. 4H). In a few cells, HIV-CFP was also observed in the nucleus when coexpressed with RHR2-YFP, but its localization was never exclusively nuclear. Coexpression of RSV-CFP and RHR2-YFP did not lead to colocalization of the fluorescent proteins or to relocalization of RHR2-YFP to the cytoplasm (Fig. 4G). Overall, these results strongly support the notion that CA is responsible for mediating the Gag-Gag interactions required to coassemble wild type Gag and chimeric Gag proteins.

The relatively low resolution of confocal fluorescence microscopy does not allow discrimination between shared sites of membrane association and direct interactions that lead to coassembly of proteins into VLPs. We decided to use correlative SEM and confocal microscopy to directly assess whether fluorescent puncta showing both fluorescent colors actually represent single particles. In this approach, cells expressing Gag were treated with EDTA to strip the cells from a gridded dish, leaving a distribution of VLPs attached to the coverslip. The fluorescence patterns of the VLPs were recorded by confocal microscopy, and then the same particles were located on the marked grid and viewed by SEM. To ensure proper assembly, cells were also transfected with nonfluorescently labeled wild-type Gag constructs at a ratio of 1:4 (fluorescent Gag: nonfluorescent Gag).

The results of this analysis agree with the colocalization data obtained by fluorescence microscopy. Pairs of Gag proteins that were observed to colocalize in DF1 cells were also observed together as individual VLPs. For example, when viewed by confocal microscopy, fluorescent VLPs from cells expressing RSV-CFP/RSV-YFP or HIV-CFP/RHR-YFP showed both fluorescent colors and were observed to be single VLPs by SEM analysis (Fig. 5A and B). However, VLPs obtained from cells expressing HIV-YFP and HRH2-CFP did not overlap in fluorescence and were observed as separate VLPs by SEM analysis (Fig. 5C). We conclude that chimeric and wild-type Gag proteins containing the same CA domain are capable of polymerizing into a single VLP. Although one report (4) suggests that plasma membrane targeting may dictate copackaging of Gag, we found no evidence for this by correlative SEM and confocal microscopy analysis (Fig. 5C). Proteins containing the same MA domain were not observed to coassemble unless they also had the same CA. In summary, all of these data firmly establish that CA is the major domain dictating Gag-Gag interactions.

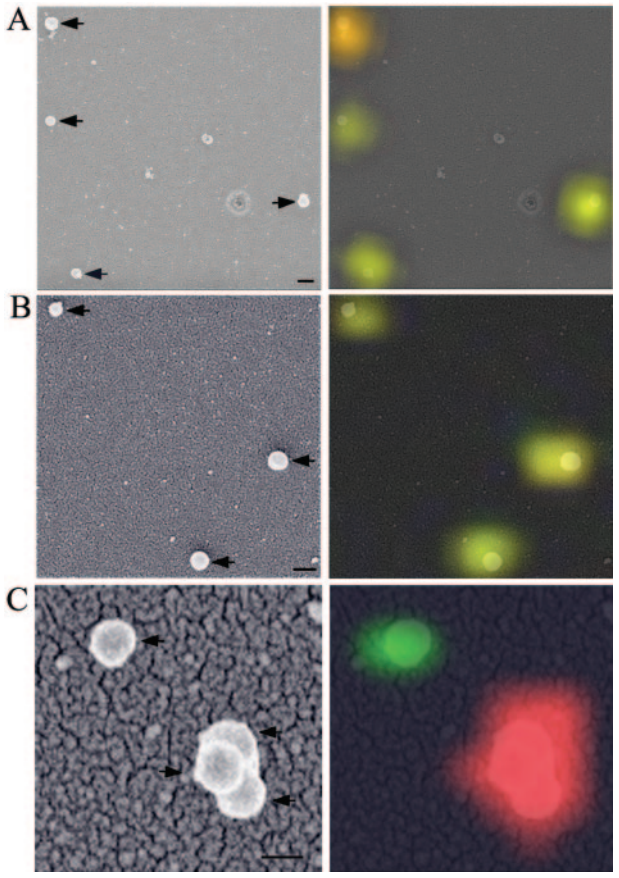


FIG. 5. Correlative SEM and confocal visualization of VLPs from fluorescent wild-type and chimeric Gag proteins from DF1 cells. (A) RSV Gag-YFP and RSV Gag-CFP. Black arrows point to VLPs in SEM images (B) HIV-1 Gag-CFP and RHR-YFP. (C) HIV-1 Gag-YFP and HRH2-CFP particles. The last panel in each row represents an overlay of the SEM and confocal images. Fluorescent images are pseudocolored (CFP = green, YFP = red) and represent a single focal plane.

## DISCUSSION

In this study, we used RSV/HIV-1 Gag chimeras to show that the CA domain is the primary determinant of VLP size and morphology, as well as the Gag-Gag interactions required for coassembly. Exchange of the NC or MA domains did not result in any significant change in the appearance of particles

FIG. 4. Fluorescence visualization of chimeric and wild type Gag proteins. Samples were prepared as in the results shown in Fig. 3. HRH2-CFP and RSV Gag-YFP (A); RSV Gag-CFP and RHR-YFP (B); HIV-1 Gag-CFP and RHR-YFP (C); HRH2-CFP and HIV-1 Gag-YFP (D); RHR2 alone (40× objective) (E); RHR2-YFP and nonlabeled HIV-1 Gag (40× objective) (F); RSV Gag-CFP and RHR2-YFP (G); RHR2-YFP and HIV-1 Gag-CFP (H). Images are pseudocolored (CFP = green, YFP = red) and represent a single focal plane.

by TEM. This lack of an effect might have been anticipated from previously published reports. Replacement of RSV NC with a dimer-forming leucine zipper led to spherical particles resembling RSV (33). Replacement of the bulk of HIV-1 MA by a short myristylated sequence resulted in spherical and infectious particles that resembled HIV-1 (59). Exchanging MA domains from different genera of retroviruses did not obviously alter the appearance of budding VLPs in insect cells (36). Our results along with these data imply that MA and NC do not contain major morphology determinants.

Exchange of the CA domains resulted in morphology and size resembling that of the parent Gag protein with the same CA. In the case of RSV CA, for the chimeric protein to assemble properly, the immediately adjacent upstream sequence of 25 amino acid residues had to be present, as inferred previously (10, 33, 35). We did not test if the short SP segment downstream of both RSV and HIV-1 CA could be exchanged. Overall, these results are consistent with reports implicating CA in assembly (12, 24, 58, 63). Previous mapping of the size determinants of retroviral VLPs to other domains of Gag used rate-zonal sedimentation (26, 27, 42). Such low-resolution methods cannot distinguish between Gag aggregates, such as those formed by the HnRc and RnHc chimeras, and morphologically distinct VLPs. TEM allowed us to directly compare wild-type and chimeric VLPs.

A hallmark of immature retrovirus particles is the dense inner ring observed in thin-section EMs. The origin of this structural feature is unknown. We hypothesize that it corresponds to the radial density attributed to the CA CTD in cryo-EM analysis or perhaps to the CTD in conjunction with the NC domain bound to RNA. The NTD and CTD densities give rise to what appears to be a p6 lattice that has been analyzed in immature HIV-1 particles (7) and more recently also in RSV particles (J. A. Briggs et al., submitted for publication). For both viruses, the Gag lattice dimensions at the CTD are similar, but the RSV lattice has a smaller radius of curvature, consistent with the TEM data for wild-type and chimeric VLPs. Furthermore, by cryo-EM the distance between what is inferred to be the NTD radial density and the MA radial density is greater in RSV than in HIV-1, presumably due to the presence of the p2 and p10 domains between MA and CA. While the TEM outer spacing measurements (Table 1) are subject to larger intrinsic errors, they are fully consonant with the more accurate cryo-EM analysis.

We found that proper assembly required the NTD and CTD to be derived from the same CA. Hydrogen-deuterium exchange and chemical cross-linking applied to in vitro-assembled HIV-1 tubes (43, 44) imply that the NTD and CTD are in close contact. In RSV, second-site suppressor analysis of mutations in the CTD also suggests such an interaction (6). However, conclusions drawn for assembly of mature CA cannot necessarily be extended to immature assembly of Gag. Thus, our findings that in the context of Gag, an NTD is compatible only with a CTD derived from the same virus support the idea that NTD-CTD contacts are essential in assembly of immature VLPs.

The chimeric Gag proteins provided a novel means of identifying the domains of Gag involved in the Gag-Gag interactions that are required for coassembly. We used fluorescently labeled versions of RSV, HIV-1, and MLV Gag proteins and of the RSV/HIV-1 chimeric Gag proteins that were found to assemble into normal VLPs in insect cells. Cells coexpressing any two different wild-type Gag proteins showed punctate fluorescence with little overlap, implying distinct sites of assembly. By contrast, cells coexpressing a wild-type Gag and a chimeric Gag showed extensive overlap of punctate fluorescence if, and only if, the Gag proteins shared the same CA domain. One possible interpretation of these findings is that RSV, HIV-1, and MLV Gag proteins each seek out different membrane sites for assembly and that such putative membrane sites are determined by CA. A different interpretation is that fluorescence colocalization reflects coassembly of different Gag proteins into the same VLPs. The observation that HIV-1 Gag-CFP causes a dramatic relocalization of RHR2-YFP from the nucleus to the cytoplasm supports the latter interpretation. It was previously reported that both fluorescent and nonfluorescent RSV Gag proteins lacking a nuclear export signal element in p10 are located predominantly in the nucleus (60). Furthermore, the normal, predominantly cytoplasmic and membrane localization of RSV Gag is rapidly changed to nuclear upon addition of the CRM-dependent export inhibitor leptomycin B (60). The most likely explanation for why HIV-1 Gag causes relocalization of the RHR2-YFP chimera to the cytoplasm is that the two proteins interact.

While RHR2-YFP was predominantly nuclear in transfected DF1 cells, RHR2 VLPs were readily detected only in the pellet of centrifuged medium from baculovirus-infected SF9 cells. It is difficult to adequately account for this discrepancy. We speculate that the high level of expression in insect cells leads to intracellular assembly of VLPs, possibly even in the nucleus, followed by cell death and liberation of the particles into the medium. The nuclei of DF1 cells expressing RHR2-YFP did not show a diffuse distribution but rather distinct, large aggregates of fluorescent puncta, which might represent assembly sites.

To directly address the hypothesis that some chimeric and wild-type Gag proteins can assemble into the same VLP, we developed a method to view individual particles both by fluorescence microscopy and by SEM. The results showed convincingly that fluorescent puncta observed in both the CFP and YFP channels corresponded with authentic VLPs (or small clusters of VLPs) made of two different Gag proteins and that this coassembly was determined by the CA domain. This conclusion is consistent with a recent report by Andrawiss et al. (2), who studied coassembly of GFP-tagged and nonfluorescent MLV Gag molecules into virions, where virions were defined simply as the fluorescent puncta adsorbed onto a coverslip. Mutations in CA prevented coassembly. In an earlier study, an HIV-1/MLV chimera was shown to be incorporated into wild-type MLV virions in a CA-dependent manner (18).

A limitation of the correlative microscopy technique is that it does not allow a sensitive quantitative estimate of the relative amounts of fluorescent Gags in an individual particle. For example, if a VLP contained >90% Gag molecules of one fluorescent color and <10% of the other, it is unlikely that the particle would be interpreted as having a mixed composition. This qualification may explain an apparent discrepancy between our data and published results on Gag proteins with the same N-termini. Bennett and Wills (4) constructed RSV Gag and MLV Gag proteins, each carrying the 10-amino-acid, myristylated sequence of the Src oncoprotein. After coexpression, the resulting VLPs shed into the medium were treated with

detergent and incubated with anti-RSV antiserum. A significant fraction of MLV Gag was found to coimmunoprecipitate with RSV Gag, and this effect required the presence of the N-terminal Src peptide on both Gag proteins. The authors interpreted this result as evidence that the primary determinant of copackaging was the membrane targeting sequence of Gag. Based on the results presented here, we speculate that if the N-terminal Src sequence plays a role in coassembly, it is minor. If even a small number of RSV Gag molecules were incorporated into mixed RSV/MLV particles, the immature virus particle might still be recognized by anti-RSV Gag antibodies, thereby leading to coimmunoprecipitation. This hypothesis remains to be examined directly by correlative microscopy.

In summary, our findings strongly support a model in which CA is the major determinant of Gag-Gag interactions. However, other Gag domains may be involved in enhancing or promoting these interactions in authentic retroviral virions. For example, by binding to several elements in the RNA packaging sequence, the NC domains could indirectly promote CA-CA interactions. This idea is consistent with the results of in vitro assembly of RSV Gag on short oligonucleotides (48), which imply that the role of NC is to induce dimerization of Gag molecules through the CA domain. An analogous argument could apply to the MA domain, in particular for viruses in which MA forms trimers, such as HIV-1 (62), or dimers, such as human T-cell leukemia virus type 1 (57). For example, a chimeric HIV-1 Gag protein carrying only the MLV MA domain was suggested to interact with MLV Gag (18). Although CA is likely to be central to Gag-Gag interactions in all retroviruses, it would not be surprising if other domains contributed to these interactions in a virus-specific way.

## ACKNOWLEDGMENTS

We thank Becky Bean and Amanda Dalton for critical reading of the manuscript, Carol Bayles for help with confocal microscopy, and Walther Mothes and Marilyn Resh for providing reagents.

This work was supported by NIH grant CA20081.

## REFERENCES

1. **Amarasinghe, G. K., R. N. De Guzman, R. B. Turner, K. J. Chancellor, Z. R. Wu, and M. F. Summers.** 2000. NMR structure of the HIV-1 nucleocapsid protein bound to stem-loop SL2 of the psi-RNA packaging signal. Implications for genome recognition. J. Mol. Biol. **301:**491–511.
2. **Andrawiss, M., Y. Takeuchi, L. Hewlett, and M. Collins.** 2003. Murine leukemia virus particle assembly quantitated by fluorescence microscopy: role of Gag-Gag interactions and membrane association. J. Virol. **77:** 11651–11660.
3. **Bennett, R. P., T. D. Nelle, and J. W. Wills.** 1993. Functional chimeras of the Rous sarcoma virus and human immunodeficiency virus gag proteins. J. Virol. **67:**6487–6498.
4. **Bennett, R. P., and J. W. Wills.** 1999. Conditions for copackaging Rous sarcoma virus and murine leukemia virus Gag proteins during retroviral budding. J. Virol. **73:**2045–2051.
5. **Bowzard, J. B., R. P. Bennett, N. K. Krishna, S. M. Ernst, A. Rein, and J. W. Wills.** 1998. Importance of basic residues in the nucleocapsid sequence for retrovirus Gag assembly and complementation rescue. J. Virol. **72:**9034–9044.
6. **Bowzard, J. B., J. W. Wills, and R. C. Craven.** 2001. Second-site suppressors of Rous sarcoma virus Ca mutations: evidence for interdomain interactions. J. Virol. **75:**6850–6856.
7. **Briggs, J. A., M. N. Simon, I. Gross, H. G. Kräusslich, S. D. Fuller, V. M. Vogt, and M. C. Johnson.** 2004. The stoichiometry of Gag protein in HIV-1. Nat. Struct. Mol. Biol. **11:**672–675.
8. **Briggs, J. A., T. Wilk, R. Welker, H. G. Kräusslich, and S. D. Fuller.** 2003. Structural organization of authentic, mature HIV-1 virions and cores. EMBO J. **22:**1707–1715.
9. **Callahan, E. M., and J. W. Wills.** 2000. Repositioning basic residues in the M domain of the Rous sarcoma virus Gag protein. J. Virol. **74:** 11222–11229.
10. **Campbell, S., and V. M. Vogt.** 1997. In vitro assembly of virus-like particles with Rous sarcoma virus Gag deletion mutants: identification of the p10 domain as a morphological determinant in the formation of spherical particles. J. Virol. **71:**4425–4435.
11. **Campos-Olivas, R., J. L. Newman, and M. F. Summers.** 2000. Solution structure and dynamics of the Rous sarcoma virus capsid protein and comparison with capsid proteins of other retroviruses. J. Mol. Biol. **296:** 633–649.
12. **Cheslock, S. R., D. T. Poon, W. Fu, T. D. Rhodes, L. E. Henderson, K. Nagashima, C. F. McGrath, and W. S. Hu.** 2003. Charged assembly helix motif in murine leukemia virus capsid: an important region for virus assembly and particle size determination. J. Virol. **77:**7058–7066.
13. **Cimarelli, A., S. Sandin, S. Höglund, and J. Luban.** 2000. Basic residues in human immunodeficiency virus type 1 nucleocapsid promote virion assembly via interaction with RNA. J. Virol. **74:**3046–3057.
14. **Conte, M. R., M. Klikova, E. Hunter, T. Ruml, and S. Matthews.** 1997. The three-dimensional solution structure of the matrix protein from the type D retrovirus, the Mason-Pfizer monkey virus, and implications for the morphology of retroviral assembly. EMBO J. **16:**5819–5826.
15. **Craven, R. C., A. E. Leure-duPree, C. R. Erdie, C. B. Wilson, and J. W. Wills.** 1993. Necessity of the spacer peptide between CA and NC in the Rous sarcoma virus Gag protein. J. Virol. **67:**6246–6252.
16. **Dalton, A. K., P. S. Murray, D. Murray, and V. M. Vogt.** 2005. Biochemical characterization of Rous sarcoma virus MA protein interaction with membranes. J. Virol. **79:**6227–6238.
17. **Deminie, C. A., and M. Emerman.** 1994. Functional exchange of an oncoretrovirus and a lentivirus matrix protein. J. Virol. **68:**4442–4449.
18. **Deminie, C. A., and M. Emerman.** 1993. Incorporation of human immunodeficiency virus type 1 Gag proteins into murine leukemia virus virions. J. Virol. **67:**6499–6506.
19. **Dupraz, P., and P. F. Spahr.** 1992. Specificity of Rous sarcoma virus nucleocapsid protein in genomic RNA packaging. J. Virol. **66:**4662–4670.
20. **Freed, E. O.** 2004. HIV-1 and the host cell: an intimate association. Trends Microbiol. **12:**170–177.
21. **Fu, W., and W. S. Hu.** 2003. Functional replacement of nucleocapsid flanking regions by heterologous counterparts with divergent primary sequences: effects of chimeric nucleocapsid on the retroviral replication cycle. J. Virol. **77:**754–761.
22. **Gamble, T. R., S. Yoo, F. F. Vajdos, U. K. von Schwedler, D. K. Worthylake, H. Wang, J. P. McCutcheon, W. I. Sundquist, and C. P. Hill.** 1997. Structure of the carboxyl-terminal dimerization domain of the HIV-1 capsid protein. Science **278:**849–853.
23. **Ganser, B. K., S. Li, V. Y. Klishko, J. T. Finch, and W. I. Sundquist.** 1999. Assembly and analysis of conical models for the HIV-1 core. Science **283:**80–83.
24. **Ganser-Pornillos, B. K., U. K. von Schwedler, K. M. Stray, C. Aiken, and W. I. Sundquist.** 2004. Assembly properties of the human immunodeficiency virus type 1 CA protein. J. Virol. **78:**2545–2552.
25. **Garbitt, R. A., K. R. Bone, and L. J. Parent.** 2004. Insertion of a classical nuclear import signal into the matrix domain of the Rous sarcoma virus Gag protein interferes with virus replication. J. Virol. **78:**13534–13542.
26. **Garnier, L., L. J. Parent, B. Rovinski, S. X. Cao, and J. W. Wills.** 1999. Identification of retroviral late domains as determinants of particle size. J. Virol. **73:**2309–2320.
27. **Garnier, L., L. Ratner, B. Rovinski, S. X. Cao, and J. W. Wills.** 1998. Particle size determinants in the human immunodeficiency virus type 1 Gag protein. J. Virol. **72:**4667–4677.
28. **Gitti, R. K., B. M. Lee, J. Walker, M. F. Summers, S. Yoo, and W. I. Sundquist.** 1996. Structure of the amino-terminal core domain of the HIV-1 capsid protein. Science **273:**231–235.
29. **Gross, I., H. Hohenberg, C. Huckhagel, and H. G. Kräusslich.** 1998. N-terminal extension of human immunodeficiency virus capsid protein converts the in vitro assembly phenotype from tubular to spherical particles. J. Virol. **72:**4798–4810.
30. **Guo, X., J. Hu, J. B. Whitney, R. S. Russell, and C. Liang.** 2004. Important role for the CA-NC spacer region in the assembly of bovine immunodeficiency virus Gag protein. J. Virol. **78:**551–560.
31. **Hermida-Matsumoto, L., and M. D. Resh.** 2000. Localization of human immunodeficiency virus type 1 Gag and Env at the plasma membrane by confocal imaging. J. Virol. **74:**8670–8679.
32. **Jin, Z., L. Jin, D. L. Peterson, and C. L. Lawson.** 1999. Model for lentivirus capsid core assembly based on crystal dimers of EIAV p26. J. Mol. Biol. **286:**83–93.
33. **Johnson, M. C., H. M. Scobie, Y. M. Ma, and V. M. Vogt.** 2002. Nucleic acid-independent retrovirus assembly can be driven by dimerization. J. Virol. **76:**11177–11185.
34. **Johnson, M. C., H. M. Scobie, and V. M. Vogt.** 2001. PR domain of Rous sarcoma virus Gag causes an assembly/budding defect in insect cells. J. Virol. **75:**4407–4412.
35. **Joshi, S. M., and V. M. Vogt.** 2000. Role of the Rous sarcoma virus p10 domain in shape determination of Gag virus-like particles assembled in vitro and within *Escherichia coli*. J. Virol. **74:**10260–10268.

36. **Kakker, N. K., M. V. Mikhailov, M. V. Nermut, A. Burny, and P. Roy.** 1999. Bovine leukemia virus Gag particle assembly in insect cells: formation of chimeric particles by domain-switched leukemia/lentivirus Gag polyprotein. Virology **265:**308–318.
37. **Khorasanizadeh, S., R. Campos-Olivas, and M. F. Summers.** 1999. Solution structure of the capsid protein from the human T-cell leukemia virus type-I. J. Mol. Biol. **291:**491–505.
38. **Kingston, R. L., T. Fitzon-Ostendorp, E. Z. Eisenmesser, G. W. Schatz, V. M. Vogt, C. B. Post, and M. G. Rossmann.** 2000. Structure and self-association of the Rous sarcoma virus capsid protein. Structure Fold. Des. **8:**617–628.
39. **Kingston, R. L., N. H. Olson, and V. M. Vogt.** 2001. The organization of mature Rous sarcoma virus as studied by cryoelectron microscopy. J. Struct. Biol. **136:**67–80.
40. **Klein, D. J., P. E. Johnson, E. S. Zollars, R. N. De Guzman, and M. F. Summers.** 2000. The NMR structure of the nucleocapsid protein from the mouse mammary tumor virus reveals unusual folding of the C-terminal zinc knuckle. Biochemistry **39:**1604–1612.
41. **Kräusslich, H. G., M. Fäcke, A. M. Heuser, J. Konvalinka, and H. Zentgraf.** 1995. The spacer peptide between human immunodeficiency virus capsid and nucleocapsid proteins is essential for ordered assembly and viral infectivity. J. Virol. **69:**3407–3419.
42. **Krishna, N. K., S. Campbell, V. M. Vogt, and J. W. Wills.** 1998. Genetic determinants of Rous sarcoma virus particle size. J. Virol. **72:**564–577.
43. **Lanman, J., T. T. Lam, S. Barnes, M. Sakalian, M. R. Emmett, A. G. Marshall, and P. E. Prevelige, Jr.** 2003. Identification of novel interactions in HIV-1 capsid protein assembly by high-resolution mass spectrometry. J. Mol. Biol. **325:**759–772.
44. **Lanman, J., T. T. Lam, M. R. Emmett, A. G. Marshall, M. Sakalian, and P. E. Prevelige, Jr.** 2004. Key interactions in HIV-1 maturation identified by hydrogen-deuterium exchange. Nat. Struct. Mol. Biol. **11:**676–677.
45. **Li, S., C. P. Hill, W. I. Sundquist, and J. T. Finch.** 2000. Image reconstructions of helical assemblies of the HIV-1 CA protein. Nature **407:** 409–413.
46. **Liang, C., J. Hu, R. S. Russell, A. Roldan, L. Kleiman, and M. A. Wainberg.** 2002. Characterization of a putative α-helix across the capsid-SP1 boundary that is critical for the multimerization of human immunodeficiency virus type 1 Gag. J. Virol. **76:**11729–11737.
47. **Liang, C., J. Hu, J. B. Whitney, L. Kleiman, and M. A. Wainberg.** 2003. A structurally disordered region at the C terminus of capsid plays essential roles in multimerization and membrane binding of the Gag protein of human immunodeficiency virus type 1. J. Virol. **77:**1772–1783.
48. **Ma, Y. M., and V. M. Vogt.** 2004. Nucleic acid binding-induced Gag dimerization in the assembly of Rous sarcoma virus particles in vitro. J. Virol. **78:**52–60.
49. **Manrique, M. L., M. L. Rauddi, S. A. Gonzalez, and J. L. Affranchino.** 2004. Functional domains in the feline immunodeficiency virus nucleocapsid protein. Virology **327:**83–92.
50. **Massiah, M. A., D. Worthylake, A. M. Christensen, W. I. Sundquist, C. P. Hill, and M. F. Summers.** 1996. Comparison of the NMR and X-ray structures of the HIV-1 matrix protein: evidence for conformational changes during viral assembly. Protein Sci. **5:**2391–2398.
51. **Matthews, S., P. Barlow, J. Boyd, G. Barton, R. Russell, H. Mills, M. Cunningham, N. Meyers, N. Burns, N. Clark, et al.** 1994. Structural similarity between the p17 matrix protein of HIV-1 and interferon-gamma. Nature **370:**666–668.
52. **Matthews, S., M. Mikhailov, A. Burny, and P. Roy.** 1996. The solution structure of the bovine leukaemia virus matrix protein and similarity with lentiviral matrix proteins. EMBO J. **15:**3267–3274.
53. **McDonnell, J. M., D. Fushman, S. M. Cahill, W. Zhou, A. Wolven, C. B. Wilson, T. D. Nelle, M. D. Resh, J. Wills, and D. Cowburn.** 1998. Solution structure and dynamics of the bioactive retroviral M domain from Rous sarcoma virus. J. Mol. Biol. **279:**921–928.
54. **Mortuza, G. B., L. F. Haire, A. Stevens, S. J. Smerdon, J. P. Stoye, and I. A. Taylor.** 2004. High-resolution structure of a retroviral capsid hexameric amino-terminal domain. Nature **431:**481–485.
55. **Muriaux, D., S. Costes, K. Nagashima, J. Mirro, E. Cho, S. Lockett, and A. Rein.** 2004. Role of murine leukemia virus nucleocapsid protein in virus assembly. J. Virol. **78:**12378–12385.
56. **Nandhagopal, N., A. A. Simpson, M. C. Johnson, A. B. Francisco, G. W. Schatz, M. G. Rossmann, and V. M. Vogt.** 2004. Dimeric Rous sarcoma virus capsid protein structure relevant to immature Gag assembly. J. Mol. Biol. **335:**275–282.
57. **Rayne, F., A. V. Kajava, J. Lalanne, and R. Z. Mamoun.** 2004. In vivo homodimerisation of HTLV-1 Gag and MA gives clues to the retroviral capsid and TM envelope protein arrangement. J. Mol. Biol. **343:**903–916.
58. **Reicin, A. S., A. Ohagen, L. Yin, S. Höglund, and S. P. Goff.** 1996. The role of Gag in human immunodeficiency virus type 1 virion morphogenesis and early steps of the viral life cycle. J. Virol. **70:**8645–8652.
59. **Reil, H., A. A. Bukovsky, H. R. Gelderblom, and H. G. Göttlinger.** 1998. Efficient HIV-1 replication can occur in the absence of the viral matrix protein. EMBO J. **17:**2699–2708.
60. **Scheifele, L. Z., R. A. Garbitt, J. D. Rhoads, and L. J. Parent.** 2002. Nuclear entry and CRM1-dependent nuclear export of the Rous sarcoma virus Gag polyprotein. Proc. Natl. Acad. Sci. USA **99:**3944–3949.
61. **Spurr, A. R.** 1969. A low-viscosity epoxy resin embedding medium for electron microscopy. J. Ultrastruct. Res. **26:**31–43.
62. **Tang, C., E. Loeliger, P. Luncsford, I. Kinde, D. Beckett, and M. F. Summers.** 2004. Entropic switch regulates myristate exposure in the HIV-1 matrix protein. Proc. Natl. Acad. Sci. USA **101:**517–522.
63. **von Schwedler, U. K., K. M. Stray, J. E. Garrus, and W. I. Sundquist.** 2003. Functional surfaces of the human immunodeficiency virus type 1 capsid protein. J. Virol. **77:**5439–5450.
64. **Wang, S. W., and A. Aldovini.** 2002. RNA incorporation is critical for retroviral particle integrity after cell membrane assembly of Gag complexes. J. Virol. **76:**11853–11865.
65. **Wilk, T., I. Gross, B. E. Gowen, T. Rutten, F. de Haas, R. Welker, H. G. Kräusslich, P. Boulanger, and S. D. Fuller.** 2001. Organization of immature human immunodeficiency virus type 1. J. Virol. **75:**759–771.
66. **Yamashita, M., and M. Emerman.** 2004. Capsid is a dominant determinant of retrovirus infectivity in nondividing cells. J. Virol. **78:**5670–5678.
67. **Yu, F., S. M. Joshi, Y. M. Ma, R. L. Kingston, M. N. Simon, and V. M. Vogt.** 2001. Characterization of Rous sarcoma virus Gag particles assembled in vitro. J. Virol. **75:**2753–2764.
68. **Zhang, Y., and E. Barklis.** 1995. Nucleocapsid protein effects on the specificity of retrovirus RNA encapsidation. J. Virol. **69:**5716–5722.
69. **Zhang, Y., H. Qian, Z. Love, and E. Barklis.** 1998. Analysis of the assembly function of the human immunodeficiency virus type 1 gag protein nucleocapsid domain. J. Virol. **72:**1782–1789.